STEM CELLS TRANSLATIONAL MEDICINE

TISSUE ENGINEERING AND REGENERATIVE MEDICINE

Intravenous Administration of Human Umbilical Cord Blood-Derived AC133+ Endothelial Progenitor Cells in Rat Stroke Model Reduces Infarct Volume: Magnetic Resonance Imaging and Histological Findings

ASM ISKANDER,[a] ROBERT A. KNIGHT,[b] ZHENG GANG ZHANG,[b] JAMES R. EWING,[b] ADARSH SHANKAR,[a] NADIMPALLI RAVI S. VARMA,[a] HASSAN BAGHER-EBADIAN,[a] MESER M. ALI,[a] ALI S. ARBAB,[a] BRANISLAVA JANIC[a]

Key Words. Tissue regeneration • Stem/progenitor cell • Angiogenesis • Umbilical cord blood • Brain ischemia

[a]Cellular and Molecular Imaging Laboratory, Department of Radiology, and [b]Department of Neurology, Henry Ford Hospital, Detroit, Michigan, USA

Correspondence: Branislava Janic, Ph.D., Cellular and Molecular Imaging Laboratory, Department of Radiology, 1 Ford Place, 2F, Box 82, Detroit, Michigan 48202, USA. Telephone: 313-874-1681; Fax: 313-874-4494; E-Mail: bjanic@rad.hfh.edu

Received April 4, 2013; accepted for publication May 13, 2013; first published online in SCTM *EXPRESS* August 9, 2013.

1066-5099/2013/$20.00/0

http://dx.doi.org/10.5966/sctm.2013-0066

ABSTRACT

Endothelial progenitor cells (EPCs) hold enormous therapeutic potential for ischemic vascular diseases. Previous studies have indicated that stem/progenitor cells derived from human umbilical cord blood (hUCB) improve functional recovery in stroke models. Here, we examined the effect of hUCB AC133+ EPCs on stroke development and resolution in a middle cerebral artery occlusion (MCAo) rat model. Since the success of cell therapies strongly depends on the ability to monitor in vivo the migration of transplanted cells, we also assessed the capacity of magnetic resonance imaging (MRI) to track in vivo the magnetically labeled cells that were administered. Animals were subjected to transient MCAo and 24 hours later injected intravenously with 10^7 hUCB AC133+ EPCs. MRI performed at days 1, 7, and 14 after the insult showed accumulation of transplanted cells in stroke-affected hemispheres and revealed that stroke volume decreased at a significantly higher rate in cell-treated animals. Immunohistochemistry analysis of brain tissues localized the administered cells in the stroke-affected hemispheres only and indicated that these cells may have significantly affected the magnitude of endogenous proliferation, angiogenesis, and neurogenesis. We conclude that transplanted cells selectively migrated to the ischemic brain parenchyma, where they exerted a therapeutic effect on the extent of tissue damage, regeneration, and time course of stroke resolution. STEM CELLS TRANSLATIONAL MEDICINE *2013;2:000–000*

INTRODUCTION

Stroke is the third leading cause of death in United States as well as one of the major reasons for serious, long-term disability [1]. Despite the significant body of work that has been reported during past decades, developing treatment that would ensure functional recovery after stroke still poses an extreme challenge. To date, the single approved acute therapy consists of intravenous (i.v.) administration of recombinant tissue plasminogen activators (rt-PAs). However, to be the most effective, rt-PAs must be administered as early as possible after the onset of symptoms, and within a very limited time window of 4.5 hours after stroke [2]. Within this period, the therapeutic efficacy diminishes over time, whereas the likelihood of serious complications, such as hemorrhage, increases. Unfortunately, in most instances of stroke, the first symptoms are not recognized, and very few patients receive urgent care within the first few hours of insult. In addition, no treatment is available that would grant functional recovery when administered in the postischemic phase [3]. Therefore, there is a pressing need for developing more effective alternative strategies, especially pertaining to expanding the time available for therapeutic intervention.

In recent years, stem/progenitor cells have been explored as a possible tool in developing new therapies for ischemic stroke. Currently available evidence from animal studies, where stem cells from various sources were used, indicates that stem/progenitor cell transplantation can improve the function of damaged brain areas under certain conditions. This improvement is achieved by replacing damaged neurons and by modulating brain regenerative processes such as inflammation, angiogenesis, myelination, and neuroprotection [3, 4]. Embryonic as well as

adult neuronal stem cells have demonstrated significant therapeutic potential when used in animal models [5, 6]. However, their limited availability and accessibility, as well as ethical concerns, hinder the therapeutic prospects of these cells. On the other hand, bone marrow (BM) and umbilical cord blood (UCB) stem/progenitor cells have been shown to differentiate, in vitro, into cells exhibiting neuronal, glial, and endothelial cell (EC) properties [7–9]; these cell types play important roles in brain repair mechanisms. Human UCB stem/progenitor cells, in particular, have previously been used in rodent stroke models, where they exhibited a therapeutic effect, even when administered within 24 hours after the stroke [10]. New evidence has reinforced the idea that UCB provides significant advantages over other stem/progenitor cell sources. Stem/progenitor cells from UCB exhibited high levels of telomerase and proliferation activity, an absence of risks for the donor, a low risk of transmitting viral infections, and high availability, and they are less likely to immunologically react against the host [11, 12]. The majority of work in animal stroke models has used a nonfractionated human umbilical cord blood (hUCB) [13] or mononuclear UCB cell fraction [14], with reported behavioral and anatomical recovery after transplantation. On the other hand, a few studies in the middle cerebral artery occlusion (MCAo) rat model also showed that transplantation of CD34+ enriched hUCB cells improved stroke-induced behavioral deficits [10]. These results indicated that selecting for a single cell type when using UCB as a transplant source may be a promising alternative strategy. In addition, these studies emphasize the importance of deciphering the mode of action of separate cell types within the heterogeneous UCB population.

Considering that angiogenesis is critical for tissue regeneration and remodeling in postischemic brain [15], UCB-derived endothelial progenitor cells (EPCs) may be a promising choice for stroke therapy. EPCs represent a minor population of precursor cells found within mononuclear cells (MNCs) in BM, peripheral blood, and UCB. We have previously demonstrated that an hUCB cell population selected and enriched by a single AC133+ stem cell marker can be long-term in vitro expanded while preserving the EPCs' characteristics. These cells, after both short and long-term culturing, stimulated tube-like structures in in vitro and in vivo Matrigel (BD Biosciences, San Diego, CA, http://www.bdbiosciences.com) angiogenesis studies [9]. We have also shown that when applied in tumor animal models, hUCB AC133+ EPCs migrated toward tumor tissue and incorporated into tumor neovasculature, and that the exhibited angiogenic properties were not affected by magnetic labeling and cryopreservation [16].

When designing stem/progenitor cell therapies, it is crucial to have at hand a noninvasive imaging method that can (a) reliably assess stroke lesion distribution, size, and changes over time; and (b) accurately monitor the administered cells' migration, tissue accumulation, and survival. Recent work has demonstrated that magnetic resonance imaging (MRI) can be successfully used to track the in vivo migration of magnetically labeled mammalian cells to organs and sites characterized by active angiogenesis [16]. Our reported method for magnetically labeling cells uses ferumoxide (Fe) and protamine sulfate (Pro), which are both Food and Drug Administration-approved agents [17]. Fe is a superparamagnetic iron oxide (SPIO) contrast agent able to saturate magnetically at low fields, resulting in an extremely high T2 relaxation rate in solution. Pro is an agent that, when mixed with Fe, enhances cellular uptake of the FePro complex and labeling efficiency in a variety of mammalian cells. Cells labeled with FePro can be imaged using T2 and T2* weighted MRI techniques, an approach whose success we demonstrated in tracking systemically administered FePro-labeled hUCB AC133+ EPCs in animal models of human glioma [16].

In this study we examined the effect of hUCB AC133+ EPCs on stroke lesion reduction, cell proliferation, angiogenesis, and neurogenesis in an MCAo rat stroke model. We used MRI to monitor the changes in ischemic lesion size and cerebral blood flow (CBF) and to detect migration and localization of systemically administered magnetically labeled hUCB AC133+ EPCs. Immunohistology analysis was used to confirm the presence of administered cells initially detected by MRI and to quantitatively assess proliferation, angiogenesis, and neurogenesis by immunostaining for Ki67, von Willebrand factor (vWF), and Nestin, respectively.

Materials and Methods

Ethics Statement

The protocol for the use of human cord blood in this study was approved by a Henry Ford Health System institutional review board (IRB). The board determined that our use of cord blood met the criteria for waiving the requirement for patient consent/authorization. The blood collection process was maintained under the IRB-approved security protocol. Animal experiments were performed according to the protocol approved by our animal care and use committee at the Henry Ford Health System.

Isolation and In Vitro Culture of hUCB AC133+ EPCs

hUCB AC133+ EPCs were isolated from the collected blood by a two-step procedure according to our previously reported method [9]. Ficoll gradient centrifugation was performed to isolate a cord blood (CB) mononuclear cell population that was enriched for AC133+ cells by immunomagnetic-positive selection using the MidiMACS system (Miltenyi Biotec, Auburn CA, http://www.miltenyibiotec.com) according to the manufacturer's protocol. Upon isolation, AC133+ EPCs were suspended in CellGro SCGM medium (CellGenix, Freiburg, Germany, http://www.cellgenix.com/) supplemented with 40 ng/ml stem cell factor, 40 ng/ml FMS-like tyrosine kinase 3, and 10 ng/ml thrombopoietin (all from CellGenix). Cells were expanded under suspension culture growth conditions with the cell concentration kept at 5×10^5 to 1×10^6 cells per milliliter. Upon determining the cell count, cells were split by adding freshly prepared media to adjust the concentration to 5×10^5 cells per milliliter and were maintained in culture for up to 30 days.

Animal Stroke Model

Sixteen male Wistar rats, weighing between 250 and 300 g (Charles River Laboratories, Wilmington, MA, http://www.criver.com), were used. Animal experiments were performed according to the protocol approved by the institutional animal care and use committee (IACUC #0963). They were housed in pairs in a temperature- and humidity-controlled room under a 12-hour light-dark cycle. Food and water were available ad libitum. The animals were randomly assigned to one of the two transplantation groups (animals receiving hUCB AC133+ EPCs [$n = 8$] and

animals receiving phosphate-buffered saline [PBS] [$n = 8$]). The stroke model was generated by transient occlusion of the middle cerebral artery (MCA) as previously described [18]. Animals were anesthetized with 2.0% isoflurane in oxygen carrier gas. Rats also received a preoperative injection of ketamine chloride (100 mg/kg, i.p.). The MCA was occluded for 2 hours using a 4.0 monofilament nylon suture with its tip rounded by heating. First, cervical incision was performed to expose the carotid arteries, after which the right external carotid artery (ECA) was dissected free, ligated, and transected. The nylon filament was introduced into the ECA stump lumen and advanced through the right internal carotid artery (ICA) toward the right anterior cerebral artery (ACA) to occlude the right MCA at its origin. Cerebral ischemia was allowed to develop for 2 hours, after which the intraluminal suture was withdrawn from the right ACA and right ICA to permit reperfusion. The wounds were closed and sutured. The rats were allowed to recover from the anesthesia and then placed back into the cages with free access to food and water. For pain control, Buprenex (Reckitt Benckiser Healthcare Ltd., Slough, U.K., http://www.rb.com) was administered as an i.p. injection, as needed, at a dosage of 2.5 mg/kg. At the end of the study, animals were euthanized using a CO_2 inhalation overdose.

Labeling of hUCB AC133+ EPCs and i.v. Administration

At days 25–30 of primary culture, AC133+ EPCs were labeled according to our previously described method [17]. In brief, cells were suspended at a concentration of 4×10^6 cells per milliliter in serum-free RPMI. First, a ferumoxide suspension (Feridex IV; Bayer-Schering Pharma, Wayne, NJ, http://pharma.bayer.com) was added to the cells at a final concentration of 100 μg/ml. Immediately thereafter, preservative-free Pro (American Pharmaceuticals Partners, Shaumburg, IL, http://www.appdrugs.com) was added in the same manner to a final concentration of 3 μg/ml. A stock solution of Pro, which is supplied at 10 mg/ml, was freshly diluted to a concentration of 1 mg/ml in distilled water at the time of use. Cells were plated in a 24-well cell culture dish (0.5 ml per well) and incubated in the presence of the FePro complex for 15 minutes at 37°C, 5% CO_2, after which complete growth medium was added (0.5 ml per well) and the labeling procedure was continued for 4 hours at 37°C, 5% CO_2. Following the FePro labeling, cells were washed two times and incubated for 30 minutes with the red fluorescent dye DiI (Molecular Probes, Eugene, OR, http://probes.invitrogen.com) at 37°C, 5% CO_2, according to the manufacturer's suggestions. After the second labeling, cells were harvested and washed two times with PBS, and 10^7 cells were i.v. administered to the Wistar rats that had undergone the MCAo surgical procedure 24 hours earlier. The control groups of animals received i.v. injection of sterile PBS. The cell labeling efficiency for FePro was determined by Prussian blue (PB) staining and by determining the intracellular iron concentration according to our published method [17]. Cells were also labeled with the red fluorescent dye DiI according to manufacturer protocol. Ten million FePro/DiI double-labeled cells were i.v. administered to the animals that had undergone the MCAo procedure 24 hours earlier. Animals in the control group received sterile PBS intravenously.

MRI

Image Acquisition

The animals were anesthetized with 1%–2.0% isoflurane in a 2:1 N_2O:O_2 gas mixture and secured to a customized cradle. The core temperature was maintained at 37.0°C. MRI was performed using a 7.0 T, 20 cm bore, superconducting magnet (Varian, Palo Alto, CA, http://www.varian.com). A tri-pilot scan imaging sequence was used for reproducible positioning of the animal in the magnet at each MRI session. In vivo multiecho T2-weighted imaging (T2WI), T1-weignted imaging (T1WI), susceptibility weighted imaging (SWI), and CBF were performed for all animals 24 hours after MCAo (before cell injection) and 7 and 14 days after cell injection using the following sequences: spin echo T2WI multislice (13 slices), multiecho (4 echoes) MRI sequence (TE = 20 ms, TR = 2,000 ms, 32 × 32 mm FOV, 1 mm slice thickness, 128 × 128 matrix, and NEX = 2), single-echo T1WI multislice (27 slices) MRI sequence (TE = 15.68 ms, TR = 800 ms, 32 × 32 mm FOV, 0.4 mm slice thickness, 256 × 192 matrix and NEX = 4), SWI MRI sequence (TE = 10 ms, TR = 25 ms, 32 × 32 × 24 mm FOV, 256 × 192 × 64 matrix and NEX = 1), and arterial spin labeling (ASL) MRI sequence (TE = 13 ms, TR = 1,500 ms, 32 × 32 mm FOV, 64 × 64 matrix and NEX = 8). MRI maps were created from the acquired images and analyzed.

MRI Data Analysis

Images acquired with T2-weighted sequences were used to generate T2 maps that were further analyzed using ImageJ (http://rsbweb.nih.gov/ij/). Irregular regions of interest (ROIs) were drawn to encircle the entire stroke lesion exhibited as hyperintensity area in each T2 map. The delineated lesion areas were summed and multiplied by the slice thickness to determine the stroke volume for each time point. The observed changes were expressed as percentage change compared with the stroke volume calculated at day 1, which was set as 100%.

CBF maps generated from ASL pulse sequences were used to evaluate changes in blood flow over time. Irregular ROIs outlining the stroke areas were created in T2 maps and were transferred horizontally to the ipsilateral side (the brain midline was used as the line of reference) of the corresponding slice CBF map. Mean value of the CBF was measured in the ipsilateral and contralateral sides using the ROIs specified in T2 maps. Mean CBF measurements obtained from the ipsilateral hemisphere were normalized to the mean CBF measurements obtained from contralateral hemisphere. Data analysis was performed in ImageJ on the maps generated at days 1, 7, and 14 after the MCAo procedure. Final processing and statistical analysis of the data were performed in GraphPad Prism (version 6 for Windows; GraphPad Software, Inc., San Diego, CA, http://www.graphpad.com).

Immunohistochemistry

Fourteen days after stroke induction, animals were sacrificed; the brain tissue was collected, fixed, and cut along the coronal plane into 2-mm-thick sections that were paraffin-embedded. Paraffin-embedded tissue sections were further processed into 6-μm slices that underwent histological analysis. 3,3′-Diaminobenzidine (DAB)-enhanced PB staining was used to confirm the presence of iron (FePro)-labeled hUCB AC133+ EPCs within the brain tissue. Fluorescence microscopy was also used to determine the presence of administered DiI fluorescently labeled cells and their proximity to the blood vessels that were visualized by

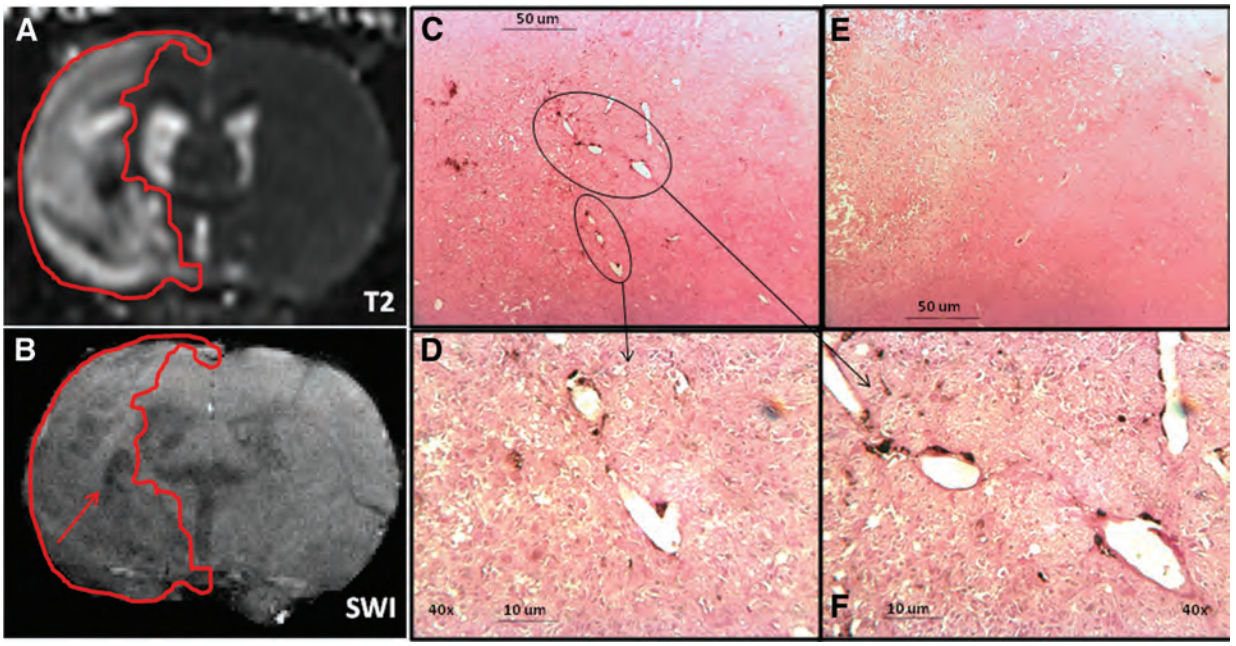

Figure 1. Tracking of ferumoxide and protamine sulfate (FePro)-labeled human umbilical cord blood (hUCB) AC133+ endothelial progenitor cells (EPCs) to brain ischemic lesions. FePro-labeled hUCB AC133+ EPCs were administered i.v. to the rats that had undergone middle cerebral artery occlusion 24 hours earlier. Fourteen days after cell administration, magnetic resonance imaging (MRI) identified stroke lesions and demonstrated the presence of administered cells within the lesions. **(A):** T2 MRI maps depicting the stroke area as a hyperintense (white) region, bordered in red. **(B):** SWI showing the accumulation of FePro-labeled cells in the stroke-affected hemisphere, within the same slice that is bordered in red in **(A)**. **(C, D, F):** 3,3′-Diaminobenzidine enhanced Prussian blue staining confirmed the accumulation of FePro-labeled cells mainly in the ischemic boundary, within and around large thin blood vessels. **(E):** No cells were detected in the brains of control animals. Magnification, ×10 **(C, E)** and ×40 **(D, F)**. Scale bars = 50 μm **(C, E)** and 10 μm **(D, F)**. Abbreviation: SWI, susceptibility weighted imaging.

fluorescein isothiocyanate (FITC)-labeled tomato Lectin (Sigma-Aldrich, St. Louis, MO, http://www.sigmaaldrich.com). To assess proliferation, angiogenesis, and neurogenesis, the following antibodies were used, respectively: polyclonal rabbit anti-rat Ki67 (Millipore, Billerica, MA, http://www.millipore.com), polyclonal rabbit anti-human vWF (Dako, Glostrup, Denmark, http://www.dako.com), and monoclonal mouse anti-rat Nestin (Millipore). Notably, anti-vWF antibody used in this procedure cross-react with rat antigens. Positive signals were visualized by using UltraVision Quanto horseradish peroxidase DAB technology for polymeric labeling (Thermo Fisher Scientific, Waltham, MA, http://www.thermofisher.com). Nuclei were counterstained with hematoxylin. Each section was digitized using bright-light ×4, ×10, and ×40 field microscope objectives (AmScope, Irvine, CA, http://www.amscope.com). Quantitative analysis was performed on the digital images by counting positive signals within five randomly chosen fields within ischemic boundary encompassing the subventricular zone (SVZ), corpus callosum (CC), and striatum (Str). The counting was performed on three separate tissue sections with a 2-mm gap between sections, and the number of positive cells was normalized to the stroke volume determined at day 1.

Statistical Analysis

Treatment group comparisons and measurements of changes over time were performed. The effect size was defined as the mean difference divided by the SD. To have a detection power for an effect size of 1.5 or greater, a sample size of $n = 8$ in each group with confidence level of 95% ($\alpha = 0.05$) were assumed. Final processing and statistical analysis of all the data were performed in GraphPad Prism (version 6 for Windows) and measures were expressed as mean ± SD. Statistical significance was determined with Student's t test, and $p < .05$ was considered significant.

Results

MRI and Histological Detection of Migration and Accumulation of hUCB AC133+ EPCs in Brain Stroke Lesions

To monitor stroke development and resolution, as well as the migration and localization of administered cells, 1, 7, and 14 days after the stroke onset animals underwent MRI. In all animals at days 7 and 14 after the MCAo procedure, T2-weighted images detected ischemic lesions that appeared as defined regions of signal hyperintensity (Fig. 1A). In addition, in animals receiving hUCB AC133+ EPCs, SWIs of the same sections revealed signal hypointensity areas that resulted from accumulation of FePro-labeled transplanted cells (Fig. 1B). Staining by PB of corresponding tissue sections confirmed the presence of administered FePro-labeled cells that accumulated mainly within the ischemic boundary (IB) of the stroke lesion (Fig. 1C, 1D, 1F). Some cells were detected within and around the walls of large thin blood vessels that were indicative of neoangiogenesis (Fig. 1D, 1F). As expected, PB staining did not detect any cells in the contralateral hemispheres of experimental animals (data not shown) or in control animals (Fig. 1E). Tissue sections were also stained with FITC-labeled tomato lectin, which detects the endothelial lining of blood vessels. Fluorescence microscopy demonstrated the presence of large, thin blood vessels within the ipsilateral brain hemisphere (Fig. 2A, 2B, green) and accumulation of transplanted,

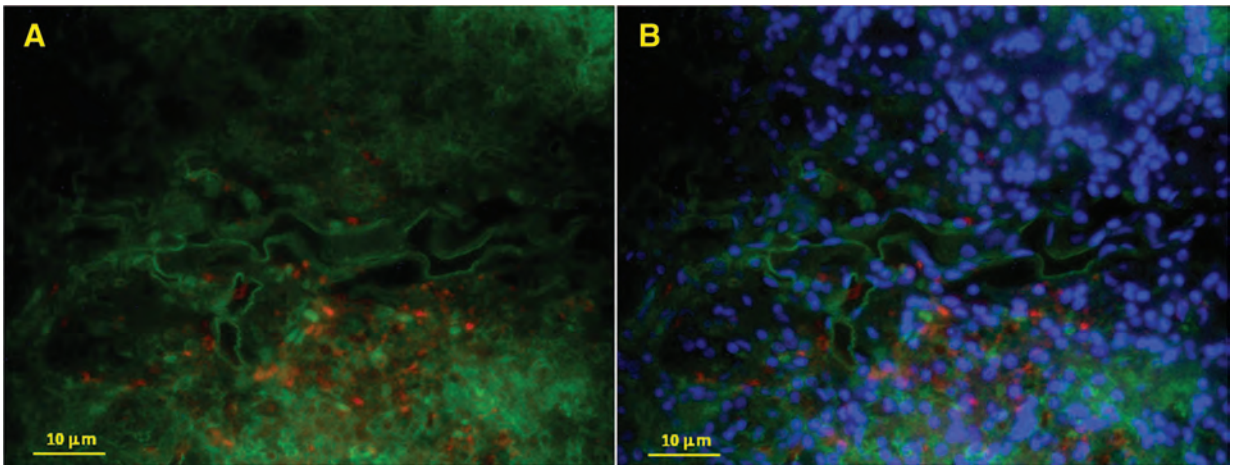

Figure 2. Detection of DiI fluorescently labeled human umbilical cord blood (hUCB) AC133+ endothelial progenitor cells (EPCs). **(A, B):** Fluorescence microscopy detected DiI-labeled hUCB AC133+ EPCs (red fluorescence) in the near proximity of large blood vessels visualized by fluorescein isothiocyanate-labeled tomato lectin (green fluorescence). Nuclei were visualized by 4′,6-diamidino-2-phenylindole (blue fluorescence). Magnification, ×40. Scale bars = 10 μm.

DiI-labeled cells that colocalized with or were in the vicinity of lectin-positive structures (Fig. 2A, 2B, red).

Changes in Stroke Volume Over Time: MRI Analysis

In addition to detecting transplanted cells, MRI was also used in evaluating changes in stroke lesions over time. In the subacute phase (24 hours after MCAo), bright zones observed on MRI were identified as ischemic lesions in both experimental and control groups. T2 maps constructed from T2-weighted images were used for measuring changes in stroke volume at different time points (Fig. 3A). Over the course of 15 days, stroke-affected areas decreased in size, and quantitative analysis demonstrated that the rate of shrinkage was higher in the animals receiving cells compared with the control animals. In the control group, stroke volume decreased by 43% at day 7, whereas in the animals receiving cells this decrease was at 34% of original volume calculated at day 1 after MCAo. Statistical analysis showed that by day 7, stroke-affected areas decreased in volume at a significantly higher rate in animals receiving cells compared with the control animals ($p < .05$). However, at day 14 after MCAo, a significant difference between control and experimental animals was not observed (Fig. 3B).

hUCB AC133+ EPCs Enhance Expression of vWF and Nestin

Brain tissue recovery after stroke is a complex, multifactorial process encompassing various self-repair mechanisms. One of the processes involved in injury resolution and tissue regeneration is neovascularization, which is closely associated with neurogenesis and neurological recovery [19]. To assess vascularization as well as neurogenesis, tissue sections were stained with anti-vWF and anti-Nestin antibodies. vWF is a marker that is expressed by mature ECs and is often used for analyzing tissue vasculature [20]. Nestin is generally considered a neural stem/progenitor cell marker [21]. On the other hand, recent studies have demonstrated Nestin expression in newly formed ECs, and as such it has been used as a reliable marker for neovascularization [22]. Analysis of tissue sections obtained from animals that received hUCB AC133+ EPCs revealed strong positivity for vWF within the ischemic core (IC) and the IB. This expression was of higher magnitude (Fig. 4A, 4C) compared with vWF expression in control animals (Fig. 4B, 4D). Quantitative analysis was performed by counting positive cells within the IB. Animals that received hUCB AC133+ EPCs exhibited significantly higher numbers of cells expressing vWF compared with the control animals (Fig. 4E). Similar results were observed with regard to Nestin expression. In addition to being expressed in IC and IB (Fig. 5A, 5B), strong Nestin activity was also observed within the ipsilateral SVZ. Interestingly, ipsilateral brain parenchyma within the SVZ and adjacent to ventricular walls exhibited stretches of Nestin-positive cells that extended toward IB and IC, giving an impression of cells migrating toward the ischemic lesion. The same pattern was not observed within the contralateral SVZ (Fig. 5D). The data showed significantly higher numbers of cells expressing Nestin in animals receiving hUCB AC133+ EPCs as compared with the control animals (Fig. 5E). Interestingly, Nestin expression was observed in cells that exhibited neuronal morphology and in cells forming vascular structures that were localized mainly within the IB. Notably, the antibody used to detect Nestin expression was specific for rat tissue, with no cross-reactivity to human antigens.

hUCB AC133+ EPCs Stimulate Proliferation of Endogenous Cells

One of the mechanisms involved in postischemic brain repair is enrichment of the endogenous progenitor cell population, which stems mainly from SVZ and hippocampal dentate gyrus and is stimulated by insults such as stroke [23]. To determine the effect of hUCB AC133+ EPCs on endogenous cell proliferation, tissue sections were analyzed for the expression of nuclear proliferation protein Ki67. Two weeks after stroke, tissue sections were stained with anti-rat Ki67 antibody and analyzed by counting the positive cells within the ipsilateral hemisphere, including the IB area of the CC (Fig. 6A, 6B), SVZ (Fig. 6A, 6C), and Str (Fig. 6A, 6D). Significantly higher numbers of proliferating cells were detected in animals treated with hUCB AC133+ EPCs compared with control animals (Fig. 6E). However, the type and origin of these proliferating could not be determined.

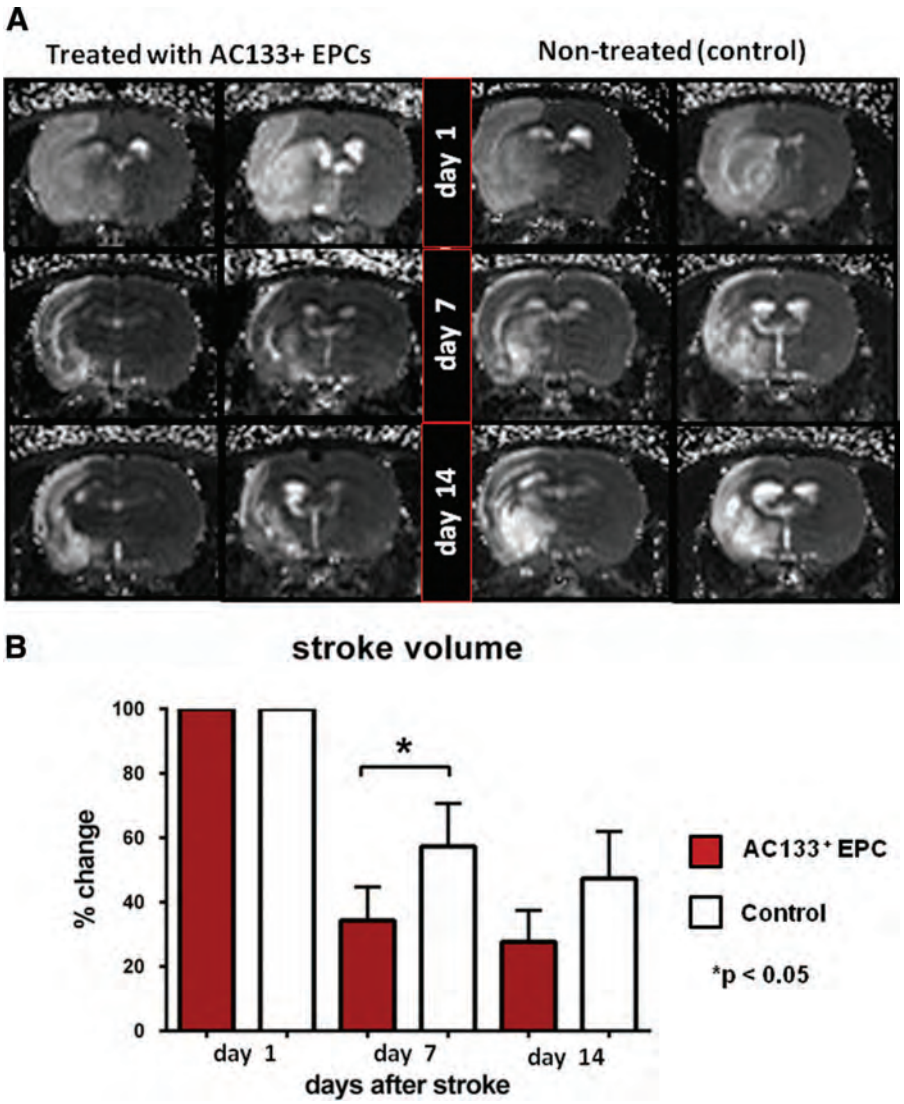

Figure 3. Changes in stroke volume over time: magnetic resonance imaging analysis. Images of T2 maps constructed from T2-weighted images depict stroke lesions as hypointense areas at days 1, 7, and 14 after middle cerebral artery occlusion in cell-treated and control animals. **(A):** Magnetic resonance T2-weighted images from two representative animals from each group (cell-treated and control). **(B):** Quantitative analysis of T2 maps revealed that over the course of 15 days, stroke-affected areas shrank at a significantly higher rate in animals that received ferumoxide and protamine sulfate-labeled human umbilical cord blood AC133+ EPCs as compared with the control animals. Graph shows mean ± SD. *, $p < .05$. Abbreviation: EPC, endothelial progenitor cell.

MRI Analysis of Cerebral Blood Flow

MRI images obtained using ASL sequences at days 1, 7, and 14 after the MCAo procedure were used to create CBF maps. Quantitative analysis demonstrated that at day 1 animals receiving hUCB AC133+ EPCs and control animals exhibited similar mean values describing blood flow in the affected hemisphere. At this time point after MCAo, CBF values in the regions of stroke defined by the corresponding T2 map (Fig. 7A, 7B) were approximately 50% of the corresponding region on the contralateral side (Fig. 7C). After 7 days CBF values exhibited a similar increase in experimental and control animals, and that increase reached approximately 80% with no difference between the groups. However, at day 14 after MCAo, CBF values of the maps generated from control animals were lower compared with the values of the maps generated from the experimental animals (78% vs. 87%, respectively). However, a statistically significant difference was not observed. It is possible that further time points after MCAo would be needed for significance to be demonstrated.

Discussion

This study was undertaken to assess the potential of hUCB AC133+ EPCs to promote tissue recovery after ischemic damage in the MCAo rat model. To our knowledge, this is the first report in which hUCB-derived stem/progenitor cells selected for the AC133+ stem cell marker and long-term in vitro expanded as a suspension EPC culture have been shown to reduce ischemic volume when magnetically labeled and systemically administered in a rodent stroke model. The use of hUCB EPCs in cell transplantation therapies was implicated as a very promising approach for various diseases due to EPCs' attribute to migrate, in vivo, to particular tissue sites characterized by active neovascularization. However, for the success of such therapy, an in vivo

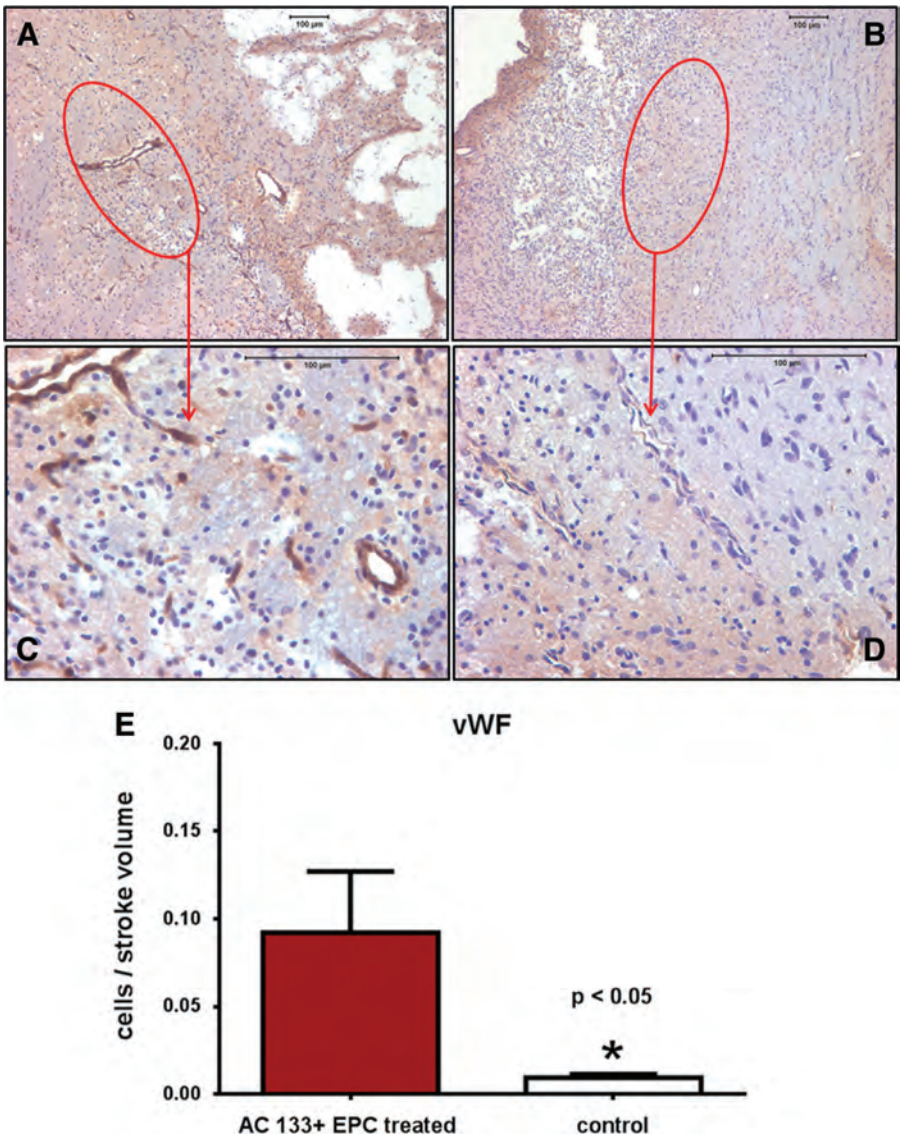

Figure 4. Expression of vascular von Willebrand factor. Anti-vWF antibody detected areas of active angiogenesis in stroke-affected hemispheres. **(A–D):** Positive signals were visualized by horseradish peroxidase 3,3′-diaminobenzidine staining. Shown are digitized sections using ×10 **(A, B)** and ×40 **(C, D)** microscope objectives. **(E):** Three coronal sections, 2 mm apart, were used for quantitative analysis performed on ×40 digital images. Significantly higher numbers of positive cells were observed in animals treated with human umbilical cord blood AC133+ EPCs compared with control animals. Magnification, ×10 **(A)** and ×40 **(B–D)**. Scale bars = 100 μm. Graph shows mean ± SD. *, $p < .05$. Abbreviations: EPC, endothelial progenitor cell; vWF, von Willebrand factor.

imaging tool that can noninvasively track the migration and accumulation of administered cells is a must. Our extensive work has demonstrated that in animal transplantation studies using stem/progenitor cells, the MRI technique in conjunction with the cellular FePro labeling method can be successfully used for in vivo tracking of the temporal and spatial migration of these cells. We previously showed that when used as an SPIO cellular labeling agent, FePro does not alter the physiology of the labeled cells [24], and it can create significant shortening of T2 and T2* relaxation times, creating a low-intensity signal that allows for administered cells to be visualized by MRI [16]. In this study, we used our recently optimized FePro labeling method [17] that enabled visualization of administered FePro-labeled hUCB AC133+ EPCs using magnetic resonance (MR) SWI sequences. These images demonstrated hypointensity areas that resulted from the accumulation of the labeled cells within the stroke lesions. These hypointensity signals were registered within the hyperintensity regions detected by MR T2 sequences, which depicted ischemic lesions within the brain. Areas of hypointensity observed by MRI correlated to the areas where iron-positive cells were detected by histological PB staining. Interestingly, the accumulation of FePro-labeled hUCB AC133+ EPCs was most prominent within the IB, with some of the cells localizing within and around the walls of large, thin blood vessels, indicative of neovascularization and previously pointed out as markers of angiogenesis in post-ischemic brain [25]. Furthermore, we confirmed the vascular and perivascular accumulation of administered cells by fluorescence microscopy, where fluorescently red cells colocalized with fluorescently green vascular structures. This observation is in agreement with earlier reports based on i.v. administration of hUCB

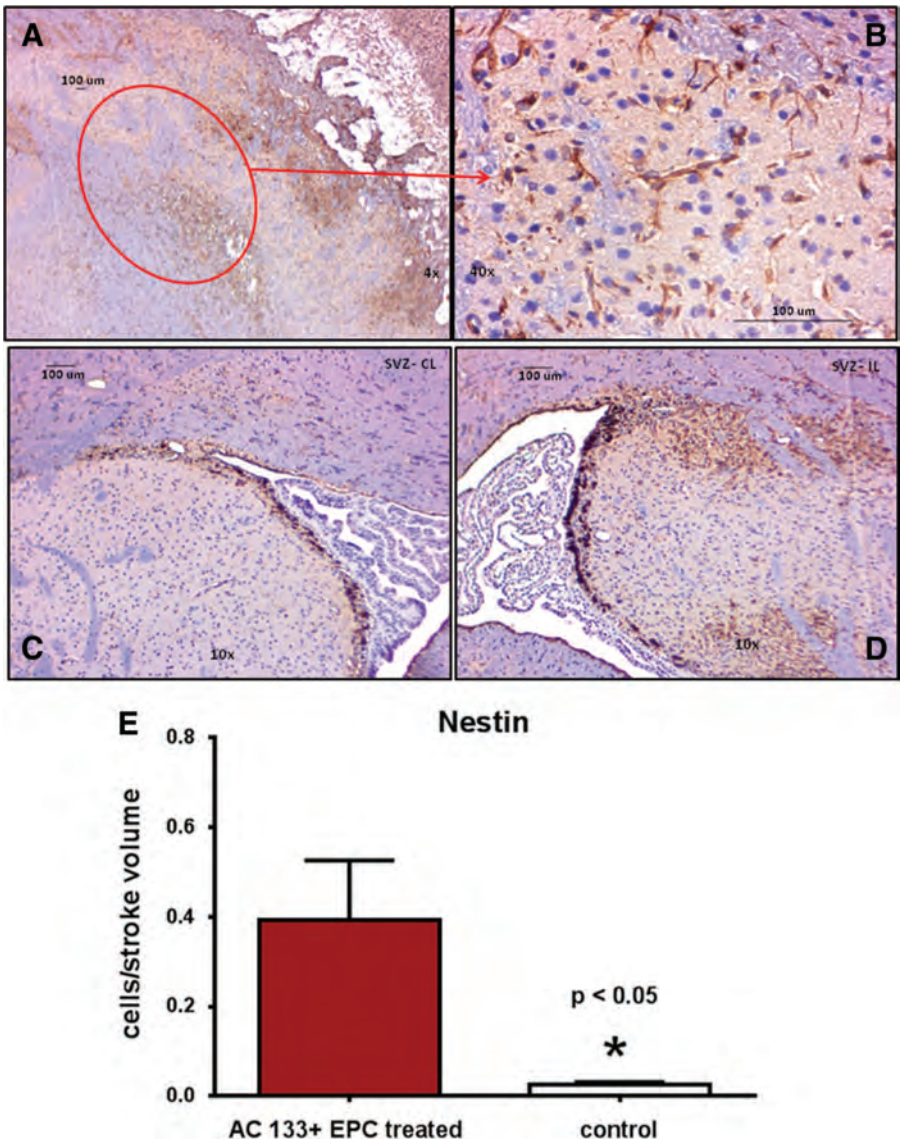

Figure 5. Expression of the neural stem/progenitor cell and neovascular marker Nestin. Anti-Nestin antibody detected areas of active neurogenesis and angiogenesis in stroke-affected hemispheres. **(A–D):** Positive signals were visualized by horseradish peroxidase 3,3′-diaminobenzidine staining. Sections were imaged with ×4 **(A)**, ×10 **(C, D)**, and ×40 **(B)** microscope objectives. **(E):** Three coronal sections, 2 mm apart, were used for quantitative analysis performed on ×40 digital images. Significantly higher numbers of Nestin-positive cells were observed in animals treated with human umbilical cord blood AC133+ EPCs compared with control animals. Magnification, ×4 **(A)**, ×10 **(C, D)**, and ×40 **(B)**. Scale bar = 100 μm. Graph shows mean ± SD. *, $p < .05$. Abbreviations: CL, contralateral; EPC, endothelial progenitor cell; IL, ipsilateral; SVZ, subventricular zone.

MNCs in a rat stroke model [13]. Most probably, i.v. injected cells follow homing signals that are in ischemic tissue conditions generated by high expression of stromal derived factor-1, a strong chemoattractant for circulating progenitors, EPCs in particular [26]. MRI tracking of stem cell migration to the ischemic brain hemispheres in rat models of stroke was reported in only a few studies; however, these studies used magnetically labeled neuronal or embryonic stem cells that were implanted locally [5, 27]. Therefore, our study provides a distinctive approach by using MRI in detecting the migration of systemically administered magnetically labeled hUCB AC133+ EPCs to the ischemic brain parenchyma.

In addition to in vivo tracking of administered cells, we have used MRI to monitor changes in the infarction volume over time. To our knowledge, this is the first report in which i.v. administration of hUCB AC133+ EPCs has been shown to significantly reduce brain ischemic volume. A significant decrease in lesion size was observed at a dose of 10^7 cells, as early as 7 days after the onset of stroke ($p = .011$). Although a similar tendency was also observed at day 14, the difference between experimental and control animals did not reach significance ($p = .052$). Similar data were reported when cells of the same type but from a different source, CD133+ human bone marrow cells, reduced stroke volume after intracerebral transplantation, but not i.v. transplantation [28]. A number of studies using the MCAo rat model have reported reduction of ischemic volume when various types of stem cells were administered systemically. In the most relevant, the application of whole hUCB cells [13] and hUCB MNCs [14] 24 hours after stroke onset exhibited neuroprotection by reducing the ischemic volume, but the significance was observed only on

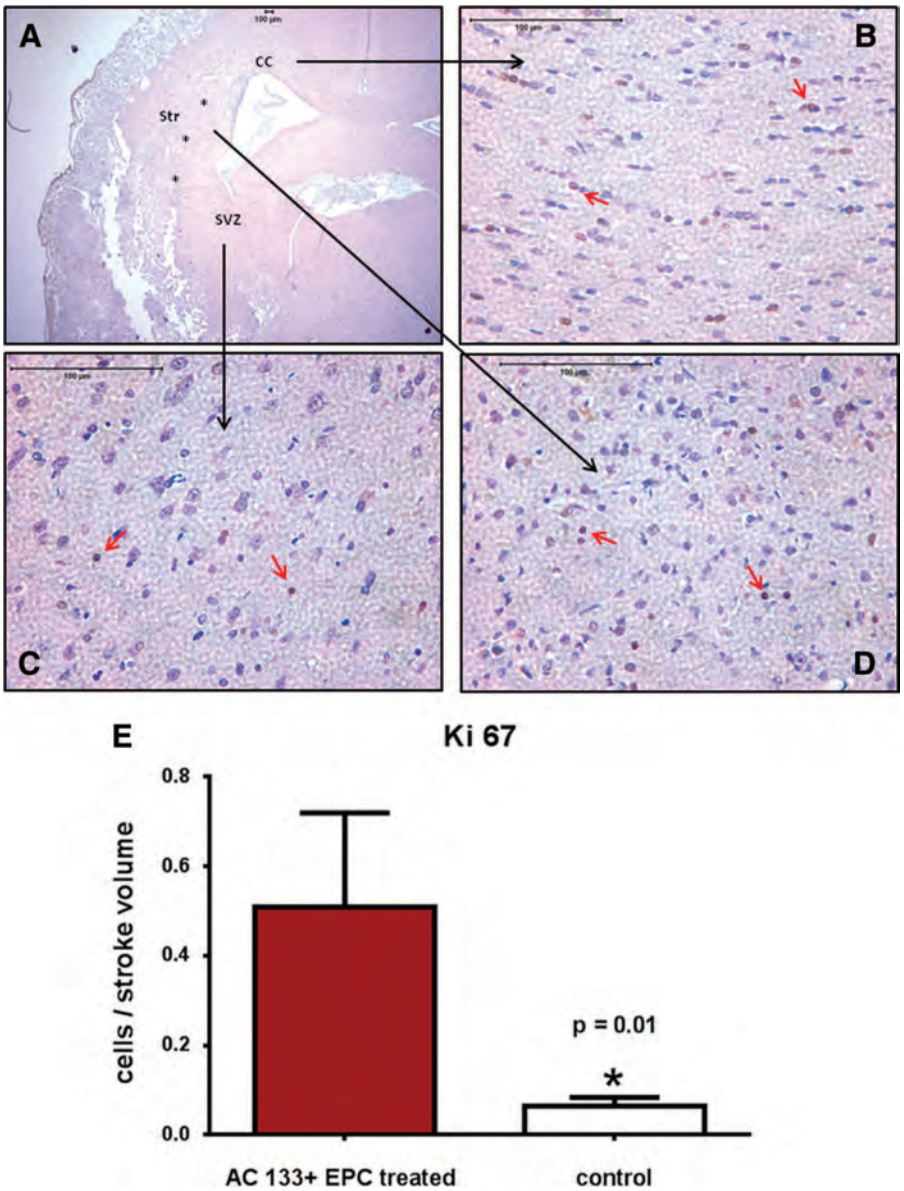

Figure 6. Expression of the nuclear proliferation marker Ki67. **(A–D):** Tissue sections stained with anti-Ki67 antibody detected proliferating cells in stroke-affected hemispheres. Ki67-positive nuclei were visualized by horseradish peroxidase 3,3′-diaminobenzidine staining (red arrows). Sections were digitized with ×4 **(A)** and ×40 **(B–D)** microscope objectives. For each animal, three coronal sections, 2 mm apart, were used for quantitative analysis performed on ×40 digital images by counting the numbers of Ki67-positive cells within the ischemic core area spanning the SVZ **(C)**, CC **(B)**, and Str **(D)**. **(E):** Significantly higher numbers of proliferating cells were observed in cell-treated animals compared with control animals. Magnification, ×4 **(A)** and ×40 **(B–D)**. Scale bars = 100 μm. Graph shows mean ± SD. *, $p < .05$. Abbreviations: CC, corpus callosum; EPC, endothelial progenitor cell; Str, striatum; SVZ, subventricular zone.

day 29. However, a study by Newcomb et al. showed that when whole hUCB cells were applied 48 hours after the insult, a decrease in the stroke lesion was observed at day 7 [29]. On the other hand, when a single CD34+ cell type was isolated from hUCB and administered systemically, despite the improvement in behavioral deficit, a reduction in stroke volume was not observed even after 25–29 days [30]. Because of the differences in experimental designs, a direct comparison between the studies cannot be made; nevertheless our findings indicate that when isolated based on AC133+ selection, hUCB-derived progenitors may have unique properties and better therapeutic potential in providing postischemic neuroprotection. In addition, this study emphasizes the importance of thoroughly analyzing separate hUCB-derived cell populations and specific administration times within the context of stroke therapy.

Mechanisms suggested in hUCB stem/progenitor cell-mediated, postischemic brain repair are neuronal rescue at the IB, cell replacement by in situ differentiation, recruitment of endogenous progenitors, and enhancement of angiogenesis, with most of these actions mediated via trophic mechanisms [31]. Angiogenic repair mechanisms have been extensively analyzed and are closely associated with neurological recovery after stroke that is most likely due to the improved vascular density and tissue perfusion around IB [25]. EPCs have been implicated to play a role in these angiogenic mechanisms. Human stroke studies revealed that within 24 hours of stroke onset, endogenous EPCs were

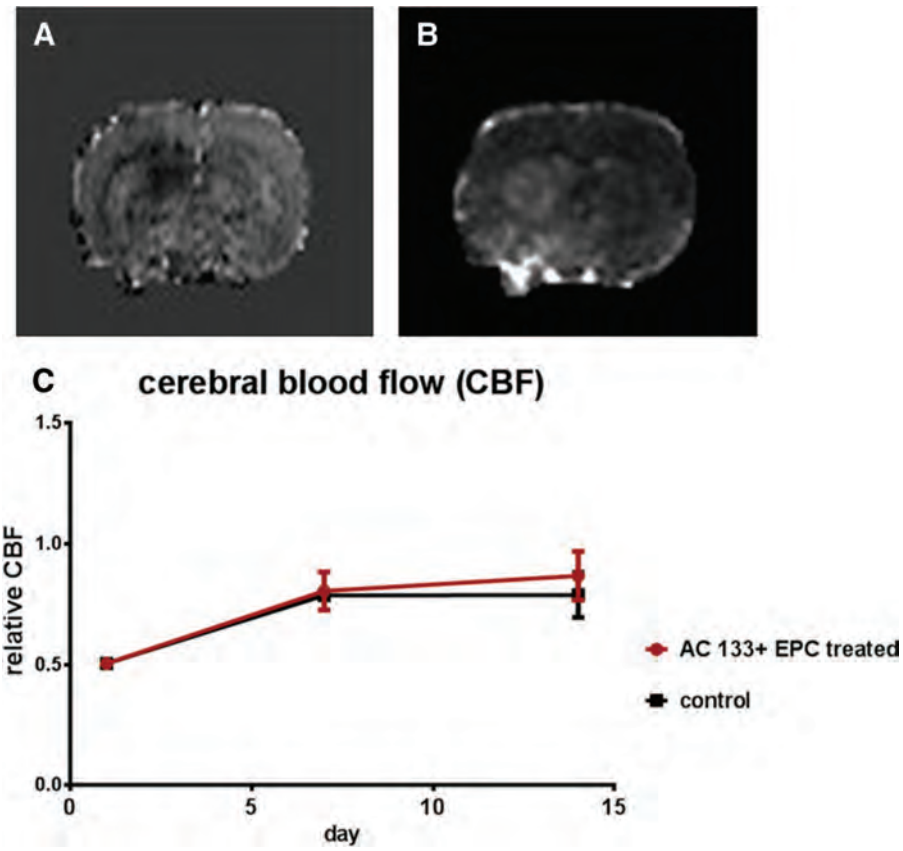

Figure 7. Effect of human umbilical cord blood AC133+ EPCs on cerebral blood flow. **(A, B):** CBF **(A)** and T2 **(B)** maps from a single representative animal taken at day 7 after the onset of stroke. **(C):** Quantitative analysis of the CBF maps revealed no significant difference in blood flow changes over the course of 15 days between treated and control groups of animals. Graph shows mean ± SD. Abbreviations: CBF, cerebral blood flow; EPC, endothelial progenitor cell.

mobilized to peripheral blood, and when isolated at later time points they exhibited greater EC differentiation and vasculogenic potential [32]. Our work showed that hUCB AC133+ EPCs exhibited angiogenic properties under in vitro and in vivo conditions that were not affected by long-term expansion [9]. Our current finding, that treatment with hUCB AC133+ EPCs significantly increases vWF expression within the IB, indicates a higher magnitude of neovascularization in treated animals and supports the concept of EPCs being an important factor in this process. However, the current experimental design was not able to decipher the origin of cells expressing vWF (human vs. rat), and therefore we could not deduce whether the administered cells underwent in situ differentiation toward ECs or whether they enhanced angiogenesis in a paracrine manner. Previous studies conceptualized the idea that new blood vessel formation is achieved by angiogenesis (proliferation and migration of adjacent structures' ECs) and vasculogenesis (EPC migration and differentiation) [33]; therefore, it is possible that both scenarios played roles in the observed effect. Our assessment of angiogenesis also included analysis of Nestin expression. In addition to being established as a neurogenic marker found in progenitors of the developing and adult central nervous system [21], recent studies demonstrated Nestin expression in endothelial precursors involved in new blood vessels formation [22]. Therefore, analysis of brain Nestin expression may give insight into the neovascularization status of the tissue. Here we found significantly higher numbers of Nestin-positive cells in animals receiving hUCB AC133+ EPCs. Interestingly, Nestin-positive cells that exhibited endothelial morphology were mostly integrated within the vasculature-like structures and mainly localized within the IB. Together, these findings indicate a higher magnitude of neoangiogenesis and neovasculogenesis in the IB of treated animals. Similarly, a significant increase in angiogenesis within the IB was reported in a rat stroke model after administration of recombinant vascular endothelial growth factor [25], which has long been established as one of the strongest angiogenic factors, with a prominent role in neovascularization [34]. Therefore, the observed hUCB AC133+ EPCs' mediated neuroprotection may be in part achieved by stimulating the growth of new blood vessels. Angiogenesis and vasculogenesis play a critical role in the post-ischemic phase and are very closely linked to neurogenesis. Besides providing a blood supply to the infarcted area, the new vasculature within the IB has also been shown to stimulate proliferation and differentiation of neuronal progenitor cells (NPCs) and to provide the scaffold for NPC migration toward ischemic lesions [35]. Interestingly, 2 weeks after the injury, our data demonstrated a prominent concentration of Nestin-positive cells within the ipsilateral SVZ, creating a pattern throughout the ipsilateral striatum indicative of cell migration toward the IB. Therefore, these Nestin-positive endogenous cells may be progenitors of neuronal origin whose spatial expansion may have been stimulated by administered hUCB AC133+ EPCs. In addition, a similar time frame after injury was previously indicated as sufficient for NPCs to migrate to ischemic areas up to 2 mm from

the SVZ [36]. Together with the subgranular zone, the SVZ has been established as a neurogenic location that responds to ischemia by a major increase in NPC proliferation and as such was shown to be the most active within the first week after ischemic insult [37]. Within that context, we analyzed the proliferation of endogenous origin by identifying cells positive for Ki67. Significantly higher numbers of proliferating cells in the treated group of animals indicate that hUCB AC133+ EPCs may have a stimulatory effect on endogenous cell proliferation that is most probably achieved by secreted factors hypothesized to have a major role in hUCB-mediated neuroprotection [38]. Considering that the number of neurons generated from proliferating endogenous NPCs is extremely low and the survival of newly differentiated neurons is very poor [39], it may be extremely important to develop strategies that can influence endogenous neuronal regeneration by expanding the endogenous pool of proliferating cells.

In addition to immunohistochemistry, we have also performed MRI analysis of CBF to indirectly assess angiogenesis. Although at day 14 after stroke we observed a tendency of hUCB AC133+ EPCs to enhance the blood flow, this trend did not reach significance. Analysis of CBF by MRI as an assessment of brain neovascularization has been successfully used before; however, in a recent study using a rat model of traumatic brain injury, a significant effect of human mesenchymal stem cell treatment was detected only in later stages (3–6 weeks) after injury [40]. Hence, further experiments, including MRI analysis at longer time periods after stroke, are necessary to fully decipher the effect of hUCB AC133+ EPCs on CBF in the postischemic phase.

Conclusion

The present study shows that treatment with systemically administered hUCB AC133+ EPCs reduces the volume of ischemic lesion in MCAo stroke model in rats. Importantly, this effect was achieved by systemically administering cells within a time frame after ischemic insult that was significantly beyond the limited window of 4.5 hours established for the single currently available therapy. Although the present study was not designed to thoroughly investigate the mechanisms involved in EPC-mediated neuroprotection, analysis of certain aspects of neoangiogenesis and neurogenesis sheds light on the mechanisms involved and indicates that modulation of these processes may be part of the observed restorative effect. Altogether, the data presented here indicate that with regard to neuroprotection under focal ischemic conditions, hUCB AC133+ EPCs may be superior to other cell types derived from CB and may offer an additional option for stroke therapy.

Acknowledgments

This work was supported by American Heart Association Grant 09SDG2230011 and by NIH Grants R01-172048 and R01-CA160216.

Author Contributions

A.I.: collection and assembly of data, data analysis, manuscript writing; R.A.K.: conception and design, manuscript writing; Z.G.Z. and M.M.A.: conception and design; J.R.E.: conception and design, data analysis and interpretation; A.S. and N.R.S.V.: collection of data; H.B.-E.: conception and design, data analysis and interpretation, manuscript writing; A.S.A.: conception and design, data analysis and interpretation, manuscript writing, financial support; B.J.: conception and design, financial support, collection and assembly of data, data analysis and interpretation, manuscript writing, final approval of manuscript.

Disclosure of Potential Conflicts of Interest

The authors indicate no potential conflicts of interest.

References

1 Centers for Disease Control and Prevention. Stroke facts and statistics. Available at http://www.cdc.gov/stroke/facts_statistics.htm. Accessed December 1, 2012.

2 Davis SM, Donnan GA. 4.5 hours: The new time window for tissue plasminogen activator in stroke. Stroke 2009;40:2266–2267.

3 Lindvall O, Kokaia Z. Stem cell research in stroke: How far from the clinic? Stroke 2011;42:2369–2375.

4 Vendrame M, Gemma C, Mesquita DD et al. Anti-inflammatory effects of human cord blood cells in a rat model of stroke. Stem Cells Dev 2005;14:595–604.

5 Hoehn M, Kustermann E, Blunk J et al. Monitoring of implanted stem cell migration in vivo: A highly resolved in vivo magnetic resonance imaging investigation of experimental stroke in rat. Proc Natl Acad Sci USA 2002;99:16267–16272.

6 Ourednik J, Ourednik V, Lynch WP et al. Neural stem cells display an inherent mechanism for rescuing dysfunctional neurons. Nat Biotechnol 2002;20:1103–1110.

7 Sanchez-Ramos JR, Song S, Kamath SG et al. Expression of neural markers in human umbilical cord blood. Exp Neurol 2001;171:109–115.

8 Sanchez-Ramos J, Song S, Cardozo-Pelaez F et al. Adult bone marrow stromal cells differentiate into neural cells in vitro. Exp Neurol 2000;164:247–256.

9 Janic B, Guo AM, Iskander ASM et al. Human cord blood-derived AC133+ progenitor cells preserve endothelial progenitor characteristics after long term in vitro expansion. PLoS One 2010;5:e9173.

10 Chen J, Sanberg PR, Li Y et al. Intravenous administration of human umbilical cord blood reduces behavioral deficits after stroke in rats. Stroke 2001;32:2682–2688.

11 Rocha V, Gluckman E. Improving outcomes of cord blood transplantation: HLA matching, cell dose and other graft- and transplantation-related factors. Br J Haematol 2009;147:262–274.

12 Gammaitoni L, Weisel KC, Gunetti M et al. Elevated telomerase activity and minimal telomere loss in cord blood long-term cultures with extensive stem cell replication. Blood 2004;103:4440–4448.

13 Vendrame M, Cassady J, Newcomb J et al. Infusion of human umbilical cord blood cells in a rat model of stroke dose-dependently rescues behavioral deficits and reduces infarct volume. Stroke 2004;35:2390–2395.

14 Boltze J, Reich DM, Hau S et al. Assessment of neuroprotective effects of human umbilical cord blood mononuclear cell subpopulations in vitro and in vivo. Cell Transplant 2012;21:723–737.

15 Fernandez MG, Fuentes B, Frutos BR et al. Trophic factors and cell therapy to stimulate brain repair after ischemic stroke. J Cell Mol Med 2012;16:2280–2290.

16 Janic B, Jafari-Khouzani K, Babajani-Feremi A et al. MRI tracking of FePro labeled fresh and cryopreserved long term in vitro expanded human cord blood AC133+ endothelial progenitor cells in rat glioma. PLoS One 2012;7:e37577.

17 Janic B, Rad AM, Jordan EK et al. Optimization and validation of FePro cell labeling method. PLoS One 2009;4:e5873.

18 Longa EZ, Weinstein PR, Carlson S et al. Reversible middle cerebral artery occlusion without craniectomy in rats. Stroke 1989;20:84–91.

19 Zhang ZG, Chopp M. Neurorestorative therapies for stroke: Underlying mechanisms and translation to the clinic. Lancet Neurol 2009;8:491–500.

20 Riedel F, Gotte K, Bergler W et al. Inverse correlation of apoptotic and angiogenic markers in squamous cell carcinoma of the head and neck. Oncol Rep 2001;8:471–476.

21 Lendahl U, Zimmerman LB, McKay RD. CNS stem cells express a new class of intermediate filament protein. Cell 1990;60:585–595.

22 Suzuki S, Namiki J, Shibata S et al. The neural stem/progenitor cell marker nestin is expressed in proliferative endothelial cells, but not in mature vasculature. J Histochem Cytochem 2010;58:721–730.

23 Kernie SG, Parent JM. Forebrain neurogenesis after focal Ischemic and traumatic brain injury. Neurobiol Dis 2010;37:267–274.

24 Arbab AS, Yocum GT, Rad AM et al. Labeling of cells with ferumoxides-protamine sulfate complexes does not inhibit function or differentiation capacity of hematopoietic or mesenchymal stem cells. NMR Biomed 2005;18:553–559.

25 Zhang ZG, Zhang L, Jiang Q et al. VEGF enhances angiogenesis and promotes blood-brain barrier leakage in the ischemic brain. J Clin Invest 2000;106:829–838.

26 Ceradini DJ, Kulkarni AR, Callaghan MJ et al. Progenitor cell trafficking is regulated by hypoxic gradients through HIF-1 induction of SDF-1. Nat Med 2004;10:858–864.

27 Daadi MM, Hu S, Klausner J et al. Imaging neural stem cell graft-induced structural repair in stroke. Cell Transplant 2013;22:881–892.

28 Borlongan CV, Evans A, Yu G et al. Limitations of intravenous human bone marrow CD133+ cell grafts in stroke rats. Brain Research 2005;1048:116–122.

29 Newcomb JD, Ajmo CT Jr., Sanberg CD et al. Timing of cord blood treatment after experimental stroke determines therapeutic efficacy. Cell Transplantation 2006;15:213–223.

30 Nystedt J, Mäkinen S, Laine J et al. Human cord blood CD34+ cells and behavioral recovery following focal cerebral ischemia in rats. Acta Neurobiol Exp (Wars) 2006;66:293–300.

31 Arien-Zakay H, Lecht S, Nagler A et al. Neuroprotection by human umbilical cord blood-derived progenitors in ischemic brain injuries. Arch Ital Biol 2011;149:233–245.

32 Navarro-Sobrino M, Rosell A, Hernandez-Guillamon M et al. Mobilization, endothelial differentiation and functional capacity of endothelial progenitor cells after ischemic stroke. Microvasc Res 2010;80:317–323.

33 Janic B, Arbab AS. The role and therapeutic potential of endothelial progenitor cells in tumor neovascularization. ScientificWorldJournal 2010;10:1088–1099.

34 Leung DW, Cachianes G, Kuang WJ et al. Vascular endothelial growth factor is a secreted angiogenic mitogen. Science 1989;246:1306–1309.

35 Kojima T, Hirota Y, Ema M et al. Subventricular zone-derived neural progenitor cells migrate along a blood vessel scaffold toward the post-stroke striatum. Stem Cells 2010;28:545–554.

36 Kokaia Z, Lindvall O. Neurogenesis after ischaemic brain insults. Curr Opin Neurobiol 2003;13:127–132.

37 Barkho BZ, Zhao X. Adult neural stem cells: Response to stroke injury and potential for therapeutic applications. Curr Stem Cell Res Ther 2011;6:327–338.

38 Borlongan C, Hadman M, Sanberg C et al. Central nervous system entry of peripherally injected umbilical cord blood cells is not required for neuroprotection in stroke. Stroke 2004;35:2385–2389.

39 Arvidsson A, Collin T, Kirik D et al. Neuronal replacement from endogenous precursors in the adult brain after stroke. Nat Med 2002;8:963–970.

40 Li L, Jiang Q, Qu CS et al. Transplantation of marrow stromal cells restores cerebral blood flow and reduces cerebral atrophy in rats with traumatic brain injury: In vivo MRI study. J Neurotrauma 2011;28:535–545.